AD NUMBER
AD079488
LIMITATION CHANGES
TO: **Approved for public release; distribution is unlimited.**
FROM: **Distribution authorized to U.S. Gov't. agencies and their contractors; Administrative/Operational Use; SEP 1955. Other requests shall be referred to Ballistic Research Lab., Aberdeen Proving Ground, MD.**
AUTHORITY
BRL ltr, 22 Apr 1981

BRL

MEMORANDUM REPORT No. 927

The Drag And Stability Properties Of The Hemispherical Base Shell, 75MM, T50E2

E. J. ROSCHKE

DEPARTMENT OF THE ARMY PROJECT No. 5B0305005
ORDNANCE RESEARCH AND DEVELOPMENT PROJECT No. TB3-0112

BALLISTIC RESEARCH LABORATORIES

ABERDEEN PROVING GROUND, MARYLAND

Destroy when no longer needed. DO NOT RETURN

B A L L I S T I C R E S E A R C H L A B O R A T O R I E S

MEMORANDUM REPORT NO. 927

September 1955

THE DRAG AND STABILITY PROPERTIES OF THE HEMISPHERICAL BASE SHELL, 75MM, T50E2

E. J. ROSCHKE

Department of the Army Project No. 5B0305005
Ordnance Research and Development Project No. TB3-0112

A B E R D E E N P R O V I N G G R O U N D, M A R Y L A N D

TABLE OF CONTENTS

B A L L I S T I C R E S E A R C H L A B O R A T O R I E S

MEMORANDUM REPORT NO. 927

EJRoschke/mjf
Aberdeen Proving Ground, Md.
September 1955

THE DRAG AND STABILITY PROPERTIES OF THE HEMISPHERICAL BASE SHELL, 75MM, T50E2

ABSTRACT

The drag and stability properties for Mach numbers from 0.7 to 1.70, of the 75mm HE shell T50E2, a hemispherical-base design, are presented and discussed. It is shown that this shell is dynamically unstable at low yaw levels for Mach numbers from 0.7 to about 1.3. It appears, however, that the behavior of this shell improves at high yaw levels at supersonic speeds. The behavior at Mach numbers between 0.7 and 0.9 is confused by apparently unstable airflows over the hemispherical base. Therefore, the aerodynamics in this speed range as inferred from an analysis of the shell's yawing motion, varies from round to round even at the same speed.

LIST OF SYMBOLS

d	Diameter of shell (unless otherwise designated), in.
K_1	Nutational Arm of Yaw, rad.
K_2	Precessional Arm of Yaw, rad.
m	Weight of shell, lb.
s	Gyroscopic Stability Factor
$\overline{s}$	Dynamic Stability Factor
A	Axial Moment of Inertia, lb. - in.^{2}
B	Transverse Moment of Inertia, lb. - in.^{2}
K_D	Drag Coefficient
K_{D_0}	Zero-Yaw Drag Coefficient
K_M	Overturning Moment Coefficient
K_L	Lift Force Coefficient
K_N	Normal Force Coefficient
K_H	Yaw Damping Moment Coefficient
K_T	Magnus Moment Coefficient
K_A	Spin Deceleration Moment Coefficient
M	Mach number
λ_1	Nutational Yaw Damping Rate, per ft.
λ_2	Precessional Yaw Damping Rate, per ft.
$\overline{\delta^2}$	Mean Squared Yaw, square degrees
δ_H	Horizontal Component of Total Yaw, rad.
δ_V	Vertical Component of Total Yaw, rad.

INTRODUCTION

Recent VT fuze tests [1] employing the 75mm, hemispherical-base shell, T50E2 as a vehicle, indicated that important performance faults of the shell itself might exist. Premature fuze functioning occurred in firings at 22.5 degrees elevation. Attempts to isolate the cause, by using different type of shell, suggested that the shell rather than the fuze is at fault. These experiments indicated that somewhere at, or near, the peak of this particular trajectory large yaws occurred and that the resulting vibrations were of sufficient magnitude to function the fuze. The velocity of the shell at the peak of a 22.5 degree trajectory is about 870 feet per second.

At the request of the fuze development people a program was initiated to study the aerodynamics of this shell in the Transonic Range facility [2], particularly at high subsonic and transonic speeds. This report discusses the results of this program.

DESCRIPTION OF SHELL

The T50E2 is a 75mm hemispherical-base shell (Fig. 1). The average physical characteristics of the shell, as fitted with either of two fuze types, are tabulated in Table I. Shell equipped with either type fuze, T73E12 or T73E7B, have approximately the same physical properties. Table II shows the variation in measured physical characteristics of several rounds of each type about the averages used for data reduction purposes. The measurements apply to completely filled shell. Several of the shell had been fired without interior examination prior to the completion of the physical measurement program; at this time it was discovered that large cavities existed in the inert filler of some of the shell. The firing program was stopped until this deficiency could be corrected. Hence there is the possibility that the data for some few of the shell were reduced using physical data that might be in greater error than indicated by Table II. All rounds were fitted with a short, pointed, steel pin in the center of the base to aid in measurement of the photographic plates.

EXPERIMENTAL PROCEDURE

The rounds were fired through the spark photographic instrumentation of the Transonic Range. This instrumentation consists of twenty-five camera stations in an enclosed firing tunnel 1120 feet long. Twelve of these stations are also equipped with 1.6 megacycle counters which permit measurements of time intervals to a least count five-eighths of a microsecond. Two photographic plates at each station (horizontal and vertical) permit a determination of the shell's attitude and position along its trajectory and the counters record the times of flight. These data can then be analyzed and fitted to determine the aerodynamic properties of the shell, [3].

The majority of the T50E2 were fired with a gun twist of 1/25 (standard). A few were fired at a twist of 1/20 from a 75mm howitzer to sample any

effects of increased spin. It was necessary to utilize some fuzes of an older type (T73E7B) in order to fuze all the available shell. Since the fuzes appeared to be very similar externally, no attempt was made to fire shell equipped with them in isolated groups. A total of 38 rounds were fired. The distribution with respect to the fuze type and twist is given below.

Gun Twist	Fuze Type	Rounds
1/25	T73E12	25
1/20	T73E12	4
1/25	T73E7B	7
1/20	T73E7B	2

During the initial firings it became evident that in order to produce sufficient yaw to yield adequate yaw and swerve reductions it would be necessary to use a yaw inducer. In the present use this consisted of a tube extension on the gun with its upper half cut away (Fig. 2). This device produces an asymmetric muzzle blast which induces yaw on an emerging shell. The yaw inducer was not used on the 75mm howitzer for the 1/20 twist tests because of installation difficulties.

EXPERIMENTAL RESULTS

General

The central problem in the treatment of the data of this program was the apparent lack of any uniquely determined trends for many of the aerodynamic properties in a Mach number range of 0.7 to about 1.2. Some of the variations which appeared seemed to arise from the effects of yaw level; others appeared to be related to flow instability over the hemispherical base. Variations of the aerodynamic properties in this region made adequate screening of the data difficult. The data are presented in the order of decreasing accuracy: drag, overturning moment, and yaw damping rates followed by the remainder of the aerodynamic coefficients. It should be noted that accuracy of determination of the drag coefficients is, statistically, on the order of tenths of a percent and that of the overturning moment coefficient usually less than one percent. However, with slight but actual differences between individual shell and the effects of yaw corrections to be considered, a scatter of say 2% for the drag coefficient and 5% for the overturning moment coefficient might be possible. The rounds of this program exhibited variations of the order of 50% in the drag at some lower Mach numbers and 10 to 20% for the overturning moment coefficient over a range of Mach numbers. This strongly suggests the shell, though physically similar, cannot be considered as aerodynamically similar in a Mach number region of 0.7 to about 0.95

Part I Drag

Fig. 3 shows the zero-yaw drag coefficient, K_{D_0}, plotted versus Mach number. The transonic drag rise of this curve is rather poorly defined but probably starts at $0.81 < M < 0.85$. Unfortunately, the three rounds fired in this speed range produced data alien to the general trend of the curve. The two relatively low yaw rounds at Mach number 0.814 developed slight, occasional shocks on the hemispherical base. The third round, at Mach number 0.852, flew the greater portion of the range accompanied by a sonic field. The source of the disturbance initiating this field appeared to be located in the wake of the shell. This is further discussed in Part II. The rise of the drag curve for $0.81 < M < .96$ is occasioned by the growth of a planar body shock and the development of body shocks issuing from the fuze, ogive, and rotating band. In the neighborhood of the Mach number 0.96 another sharp rise in the drag occurs due to the appearance of strong wake shocks. The drag curve has a typical trend, the peak lies between Mach numbers of 1.1 and 1.2 and is followed by a normal supersonic decrease.

Overturning Moment

The gyroscopic stability factor, s, is seldom less than 1.7 for 1/25 twist over the entire speed range tested, hence the behavior of the overturning moment is in a sense academic. It is interesting to note however, that this fundamentally well determined coefficient appears to be uniquely determined only above Mach number 1.1 (Fig. 4). For the region $0.7 < M < 1.1$ the values of K_M spread over a band which attains a width of about 0.3. The following poorly determined trends appear:

a. Increased yaw seems to increase K_M particularly for $0.9 < M < 1.2$.

b. Increased spin tends to increase K_M.

For the region $0.7 < M < 1.0$ the picture is quite confused.

Yaw Damping

Values of λ_1 and λ_2 are depicted in Figs. 5 and 6 as functions of Mach number. Curves for several yaw levels have been faired through the data. Note that the point distribution for the nutational damping rate, λ_1, indicates negative damping throughout the subsonic region regardless of the generally poor determination of this parameter. The precessional damping rate of the T50E2 shell, λ_2, is the more influential of the rates at transonic speeds. In Fig. 6 it can be seen that the precessional component shows a markedly negative damping rate for approximately $0.8 < M < 1.1$ and that maximum negative damping occurs at about Mach number 1.05. While negative damping of course produces greater yaw, note in Fig. 6 that the damping rates are less negative as the yaw level increases, at least for Mach numbers greater than 1.0.

It may be of interest to mention that rounds 3086 and 3087 ($1.03 < M < 1.07$) both had spiral yaw within the length of the observed range. Both rounds had small nutational arms but growing precessional arms. Fig. 7 shows the polar yaw plot of one of these rounds. The amplitude of the nutational component is very small whereas the precessional component is markedly divergent. The later portion of the curve shows some tendency that the spiral has or is approaching a maximum level of about 17 square degrees. These rounds would be expected to have large, negative values of λ_2 (Fig. 6).

Dynamic Stability

It is difficult to describe the dynamic stability of this shell completely. The qualitative picture is clear but the details are not. Individually, the majority of the rounds may be definitely classed as stable or unstable although there are doubtful cases. The results of this program indicate that dynamic stability of the T50E2 is dependent on yaw as well as Mach number. It is not possible, however, to precisely determine at what yaw the crossover between instability and stability occurs for the shell at any given Mach number.

The usually convenient condition for dynamic stability, $0 < \bar{s} < 2$, [4] where,

$$\bar{s} = \frac{2\left[K_L - \frac{md^2}{A} K_T\right]}{K_L + \frac{md^2}{B} K_H - \frac{md^2}{A} K_A}$$

cannot be applied to most of our shell. This is the case because the necessary condition for the criterion above,

$$K_L + \frac{md^2}{B} K_H - \frac{md^2}{A} K_A > 0$$

is not satisfied for the majority of the shell due to their large, negative values of K_H. Examination of Table IVa and IVb shows that just four rounds of the entire program were definitely stable and have significant values of $\bar{s}$. Of the remaining shell, seven are marginal or doubtful rounds and the rest are unstable. It is equally possible that these doubtful rounds are stable or unstable. Four of these seven rounds have values of $\bar{s}$ less than 15% removed from a critical bound value ($0 < \bar{s} < 2$). These rounds also have errors in $\bar{s}$ sufficient to compensate for the difference and hence have arbitrarily been designated as S?, possibly stable. The situation for the other three rounds is much the same, except that their values of $\bar{s}$ are very poorly determined and are greater than 50% removed from a critical bound value. These three rounds have been arbitrarily designated as U? probably unstable.

No meaningful plot containing $\bar{s}$ could be made with just four significant values of this factor. Fig. 8 therefore, deserves careful attention. The Mach number and mean squared yaw of each round have been plotted against one another. Each point is designated as to stability: either stable, doubtful, very doubtful, or unstable. The corresponding areas of instability are roughly shown as determined by the trends of the data. Above Mach number 1.0 it appears that yaw levels exist for which the shell is stable; yaw levels of six degrees or more might be required. Some types of dynamic instability can be eliminated by using higher spins. However, the nature of the instability in the present case is such that increased spin, however large, would not alter the result.

It is to be noted that the extent of the unstable region is such that the 22.5° trajectory exposes the shell to highly adverse conditions. The shell passes through most of the unstable region as it approaches the peak of the trajectory and then must retraverse this region as it accelerates on the downward leg.

Lift

The lift coefficient, K_L, is plotted as a function of Mach number in Fig. 9. No definite trend exists below Mach number 1.0 with the exception of the central curve. A trend for this curve, for mean squared yaw values between ten and twenty square degrees, exists down to about Mach number 0.9. Again, as with K_M, the subsonic region is best shown as an area of variation since no apparent trend exists. Variation with yaw level above Mach number 1.1 is slight. The peaks of the curves have been shown in the region $0.9 < M < 0.95$ but the nature of the data in this region is not sufficient to substantiate this with assurance.

Yaw Damping Moment

A glance at Fig. 10 will readily show the poor determination of K_H. Well established trends for the higher yaw levels exist above Mach number 1.1 but the entire subsonic region is obscure due to a large amount of scatter. Qualitatively speaking however, several facts are clear regarding yaw damping moment:

a. There is a large negative damping moment below Mach number of about 1.1.

b. The trends of the curves for higher yaw levels indicate about zero damping moment in the vicinity of Mach number 1.3 and a positive damping moment in the supersonic region beyond.

Note that the unstable region depicted in Fig. 8 agrees in a measure to this; the boundary of the unstable region extends up to about Mach number 1.3 and the region of probable instability beyond this. It is also clear that high levels of yaw are necessary for stable performance below Mach number 1.3.

Magnus Moment

Again with K_T, a large amount of scatter exists below Mach number 0.9. This whole general region has been depicted in Fig. 11 as an area of uncertainty to the extent, that no boundaries have been shown such as with K_M and K_L. The trends of the data are fairly clear above Mach number 1.05 but the picture for the region $0.9 < M < 1.05$ is not so clear. The peaks of the curve appear to lie in the region $1.0 < M < 1.05$.

Part II Flow Phenomena

Figs. 12, 13, and 14 are shadowgraphs of the T50E2 in flight at various Mach numbers. The pictures are self descriptive. Note the strong shock patterns at transonic velocities.

Fig. 15a is a shadowgraph of round 3099 in flight and is of particular interest. The sonic field seen in this picture was probably generated by a powerful, oscillatory wake. This round possessed abnormally high drag as previously discussed but, in addition, its remaining coefficients were also abnormal.

Fig. 15b shows an enlarged view of a typical wake. This oscillating type wake was often broken into sporadic bursts of large scale turbulence. Figs. 16a and 16b show the wakes of two different rounds which flew at approximately the same Mach number. The round shown in Fig. 16a had what is usually considered a normal wake while the comparison round in Fig. 16b had a wake of the oscillating type.

The importance of the flow phenomena associated with the hemispherical base of the T50E2 cannot be minimized. Though far from being understood, it nevertheless did cast some light on the data compiled in this program. Smooth wakes were the exception rather than the rule. A large number of the low yaw rounds possessing oscillatory wakes also developed large, negative yaw damping coefficients at subsonic and transonic speeds (Fig. 10). The greatest frequency of occurrence of turbulent, oscillatory wakes appeared in the high subsonic and transonic rounds. The tendency towards oscillatory wakes appeared to decrease greatly in the supersonic region.

CONCLUSIONS

There is little doubt that the T50E2 shell possesses undesirable subsonic and transonic characteristics. The critical velocity region for this shell covers at least the region $0.9 < M < 1.2$ and is possibly more inclusive than this. In this velocity region the shell possesses negative yaw damping and shows strong tendency towards dynamic instability at low yaw levels. For most Mach numbers in this region, an average yaw level of six or more degrees might be required to attain stability. At supersonic speeds however, relatively small yaws suffice.

Conditions at the peak of a 22.5^{o} (elevation) trajectory are unfortunately conducive to the conditions mentioned above, since the shell decelerates to subsonic speed approaching this point. At the peak, moreover, the spin in radians per caliber of travel is of the order of 0.40 corresponding to an approximate twist of 1/15. The possibility remains that high rates of spin may adversely affect the flow and consequently the performance of the shell although the limited number of rounds fired at a 1/20 twist in this program did not show appreciable performance differences from the 1/25 twist.

Flow conditions appear to be greatly affected by the hemispherical base. The initiation of a highly turbulent wake may trigger the appearance of a new type of flow condition adversely affecting the performance of the shell. Turbulent wakes, especially of the oscillatory type, were frequently detected for transonic shell in this program.

In view of these effects, it appears that this shell is capable of developing large yaws during periods of dynamic instability such as may occur at or about the peak of a 22.5^{o} trajectory. How such yawing motions may cause a malfunctioning of the VT fuze is beyond the scope of this report. However, the same fuze tested in square-based shell under identical conditions showed markedly improved behavior [1] .

Clearly, bad aerodynamics of the T50E2 is associated with its hemispherical base. Therefore, shell designers, in order to avoid trouble, should not use hemispherical base on shell which might fly at velocities below about Mach number 1.5.

REMARKS

During the analysis of the data presented in the report it became evident that additional firings were desirable to clarify the shell's properties at high subsonic speed. These firings were initiated by the author. Before these added data became available the author completed his military service and left the laboratories. The data were analysed by members of the Free Flight Aerodynamics Branch, Exterior Ballistics Laboratory, and appended to the report in Tables III C and IV C and in the graphs. Since the inclusion of the newer data did not materially alter the picture presented by the earlier results the contents and the curves of the report were not changed.

The use of the mean squared yaw as a variable to show the non-linearities of the areodynamic forces and moments is not strictly correct. In the case of shell motions involving small non-linearities which are fitted by linearized theory, the output fitting parameters are functions of various yaw factors. In the present case the correlations of the parameters with yaw had so many exceptions that the single variable $\overline{\delta^2}$ was selected to show the representative trends.

ACKNOWLEDGMENT

I wish to thank Mr. L. C. MacAllister of the Free Flight Branch for seeing this report through to publication after I have left the Ballistic Research Laboratories.

E. J. ROSCHKE

BIBLIOGRAPHY

1. Foley, H. W., Stoltman, S.P., T73E12 Fuze Performance, Status of Investigation to Determine the Cause of Decreased Operability Since June 1954, (Summary report on proximity fuzes), Eastman Kodak EK-NOD-IM-1778; 28 Oct 54 (CONFIDENTIAL).

2. Rogers, W.K., The Transonic Free Flight Range, BRL Report 849, Feb 53.

3. Murphy, C.H., Data Reduction for the Free Flight Spark Ranges, BRL Report 900, Feb 54.

4. Murphy, C.H., On Stability Criteria of the Kelly-McShane Linearized Theory of Yawing Motion, BRL Report 853, April 1953.

TABLE I

Average Physical Measurements of Shell Fitted With Two Fuze Types

Pertains to Fig. 1, all dimensions in inches

	T73E12 Fuze	T73E7B Fuze
a	14.552	14.567
b	13.312	13.224
c	0.877	0.856
d	4.695	4.640
e	6.552	6.633
f	3.728	3.732
g	0.430	.440
h	2.946	2.946
i	2.386	2.393
Wt (lb.)	12.290	12.330
c.g. (in. from nose)	8.696	8.820
A (lb. - $in.^2$)	15.146	15.385
B (lb. - $in.^2$)	143.000	148.000

TABLE II

Total Variation of Measured Rounds From Values Used for Data Reduction

	T73E12 Fuze (3 rds measured) Per Cent	T73E7B Fuze (2 rds measured) Per Cent
Wt. (lb.)	0.24	0.16
c.g. (in. from nose)	0.25	0.10
A (lb. - $in.^2$)	0.72	0.12
B (lb. - $in.^2$)	1.12	0.14

TABLE IIIa

Tabulated Data for Rounds Having 1/25 Twist

Round	M	$\overline{\delta^2}$ (square degrees)	K_D	$\lambda_1 \times 10^3$ (1/ft.)	K_1 (rad)	$\lambda_2 \times 10^3$ (1/ft.)	K_2 (rad)	K_M	s
3091*	.702	12.0	.0751	.73	.042	.40	.041	1.463	1.83
3093	.720	14.7	.0813	- .36	.040	- .20	.053	1.508	1.78
3094*	.764	23.1	.0867	- .29	.070	1.14	.044	1.534	1.77
3092	.773	34.1	.0974	- .45	.063	- .17	.080	1.428	1.87
3075	.814	7.4	.0807	- 1.24	.007	- 1.44	.043	1.390	1.90
3076	.814	7.2	.0861	- .64	.007	- 1.82	.040	1.350	1.93
3083*	.886	4.1	.0850	.94	.001	- 1.52	.033	1.513	2.14
3084	.886	5.4	.0883	.70	.013	- 1.41	.035	1.368	1.94
3073	.905	8.7	.0923	- 9.19	.001	- .54	.051	1.914	2.52
3077	.912	13.9	.1016	- .49	.014	- .35	.063	1.419	1.85
3081*	.954	6.5	.1030	- 1.34	.008	- 1.13	.042	1.398	1.89
3082	.960	6.2	.1084	.20	.007	- 1.36	.040	1.415	1.86
3071	.973	5.6	.1190	.29	.008	- 1.59	.037	1.362	1.90
3072	.985	8.7	.1415	- 1.29	.008	- 1.43	.046	1.529	1.87
3070	1.003	18.8	.1694	.32	.024	- .94	.069	1.549	1.76
3085*	1.003	10.0	.1659	.58	.004	- 1.55	.050	1.451	1.84
3090	1.029	31.9	.1930	.58	.051	- .19	.084	1.540	1.78
3086*	1.035	10.0	.1717	- 1.07	.005	- 1.84	.049	1.496	1.80
3087*	1.063	10.4	.1766	- .95	.004	- 1.37	.052	1.509	1.86
3089	1.076	11.8	.1890	1.24	.019	- 1.69	.054	1.520	1.86
3068	1.086	23.8	.2008	.40	.042	- .47	.073	1.550	1.75
3067	1.129	13.8	.1921	.39	.033	- .39	.055	1.604	1.78
3062	1.201	23.2	.1960	.56	.042	- .12	.072	1.616	1.76
3060	1.284	29.0	.1987	.67	.048	- .04	.080	1.641	1.75
3061	1.289	13.4	.1891	.37	.031	- .19	.056	1.589	1.78
3056	1.492	4.1	.1685	3.33	.002	- 1.01	.034	1.754	1.94
3058	1.705	22.9	.1731	.94	.050	.26	.066	1.649	1.73
3059	1.707	12.9	.1654	.91	.033	.00	.053	1.643	1.74
3049	2.072	negligible	.1359						
3055	2.115	negligible	.1333						
3054	2.510	3.2	.1242						
3050	2.516	1.7	.1216						

* T73E7B Fuze

TABLE IIIb

Tabulated Data For Rounds Having 1/20 Twist

Round	M	$\overline{\delta^2}$ (square degrees)	K_D	$\lambda_1 \times 10^3$ (1/ft.)	K_1 (rad)	$\lambda_2 \times 10^3$ (1/ft.)	K_2 (rad)	K_M	s
3101	.752	6.6	.0701	- 2.00	.015	- .69	.040	1.577	2.62
3100*	.792	6.8	.0690	- .93	.009	- 1.12	.043	1.620	2.56
3099	.852	1.9	.1020	- 1.43	.015	1.38	.017	1.649	2.46
3098*	.897	7.2	.0834	9.06	.001	- .74	.046	1.452	2.95
3102	.920	3.1	.0888	- 1.64	.018	- 1.08	.024	1.484	2.55
3103	.952	4.8	.0999	.01	.019	- 1.19	.031	1.554	2.78

* T73E7B

TABLE IIIc

Data From Additional Firings, 1/25 Twist

Round	M	$\overline{\delta^2}$ (sq deg)	K_D	$\lambda_1 \times 10^3$ (1/ft.)	K_1 (rad)	$\lambda_2 \times 10^3$ (1/ft.)	K_2 (rad)	K_M	s
3454	.688	7.9	.0730	.66	.026	- .86	.040	1.429	1.89
3445	.739	18.0	.0855	- .62	.037	- .60	.063	1.452	1.81
3446	.765	14.9	.0898	.07	.027	- .84	.060	1.392	1.87
3453									
3452	.834	11.5	.0906	- .73	.015	- 1.05	.055	1.300	1.97
3451	.908	11.5	.0930	- .16	.036	- .48	.046	1.408	1.89
3450	.974	15.8	.1182	.33	.024	- .78	.064	1.497	1.76
3449	1.056	29.2	.1947	.47	.053	- .18	.078	1.502	1.81
3448	1.368	14.9	.1838	.51	.039	- .25	.054	1.592	1.73
3447	1.537	21.1	.1785	.86	.047	.11	.064	1.587	1.73

TABLE IVa

Tabulated Data for Rounds Having 1/25 Twist, (Cont)

Round	M	$\overline{\delta^2}$ (square degrees)	K_L	K_N	K_H	K_T	$\frac{}{s}$ *
3091	.702	12.0	.74	.82	3.54	- .09	.82
3093	.720	14.7	.82	.90	- 3.17	.21	U
3094	.764	23.1	.74	.83	2.12	- .24	S?
3092	.773	34.1	.85	.95	- 3.45	.21	U
3075	.814	7.4	.86	.94	-10.96	.67	U
3076	.814	7.2	1.05	1.14	-10.45	.10	U
3083	.886	4.1	.80	.89	- 3.28	.58	U
3084	.886	5.4	.84	.93	- 3.73	.54	U
3073	.905	8.7	1.04	1.14	.00	.74	U
3077	.912	13.9	.96	1.06	- 4.42	.29	U
3081	.954	6.5	1.17	1.28	-10.93	.63	U
3082	.960	6.2	1.10	1.21	- 5.74	.59	U
3071	.973	5.6	.88	1.00	- 6.00	.63	U
3072	.985	8.7	1.00	1.11	-11.42	.69	U
3070	1.003	18.8	.90	1.07	- 3.64	.42	U
3085	1.003	10.0	.87	1.04	- 5.02	.61	U
3090	1.029	31.9	.83	1.03	.09	.15	S?
3086	1.035	10.0	.83	1.01	-12.25	.80	U
3087	1.063	10.4	.85	1.03	-10.11	.64	U
3089	1.076	11.8	.88	1.07	- 2.99	.61	U
3068	1.086	23.8	.86	1.06	- 1.66	.26	U?
3067	1.129	13.8	.84	1.03	- 1.33	.23	U?
3062	1.201	23.2	.83	1.03	.27	.14	S?
3060	1.284	29.0	.88	1.08	.90	.11	.14
3061	1.289	13.4	.91	1.10	- .99	.20	U?
3056	1.492	4.1	1.09	1.28	6.98	.30	S?
3058	1.705	22.9	1.01	1.18	2.90	.01	.61
3059	1.707	12.9	1.06	1.23	1.76	.10	.30

* Note: U denotes unstable, S? possibly stable, U? probably unstable.

TABLE IVb

Tabulated Data For Rounds Having 1/20 Twist, (Cont)

Round	M	$\overline{\delta^2}$ (square degrees)	K_L	K_N	K_H	K_T	$\bar{s}$ *
3101	.752	6.6	1.08	1.15	-10.99	.47	U
3100	.792	6.8	.96	1.03	- 8.89	.56	U
3099	.852	1.9	.73	.84	- 1.18	-.29	U
3098	.897	7.2	1.02	1.11	29.12	.08	U
3102	.920	3.1	1.11	1.20	-11.24	.59	U
3103	.952	4.8	.99	1.09	- 5.58	.55	U

* Note: U denotes unstable, S? possibly stable, U? probably unstable.

TABLE IVc

Data From Additional Firings

Round	M	$\overline{\delta^2}$	K_L	K_N	K_H	K_T	$\bar{s}$ *
3454	.688	7.9	.81	.88	- 1.90	.36	U
3445	.739	18.0	.82	.91	- 5.79	.36	U
3446	.765	14.9	.88	.97	- 4.19	.40	U
3453							U
3452	.834	11.5	.91	1.00	- 8.04	.53	U
3451	.908	11.5	.89	.98	- 3.73	.30	U
3450	.974	15.8	.92	1.04	- 3.10	.37	U
3449	1.056	29.2	.83	1.03	- .28	.16	S
3448	1.368	14.9	.93	1.12	- .57	.19	S
3447	1.537	21.1	.96	1.14	2.12	.06	S

* Note: U denotes unstable, S, denotes stable

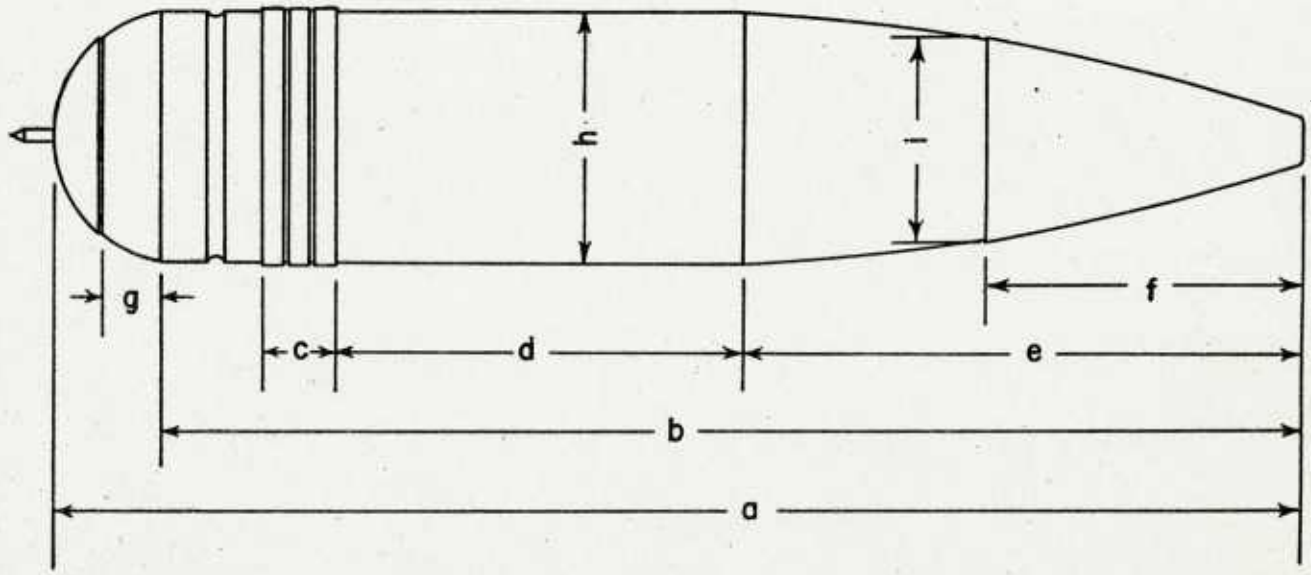

DESIGNATED DIMENSIONS ARE GIVEN IN TABLE I

75 mm SHELL, T 50-E 2

FIG 1

FIG. 2. 75MM GUN EQUIPPED WITH YAW INDUCER.

ZERO-YAW DRAG FORCE COEFFICIENT
VS
MACH NUMBER

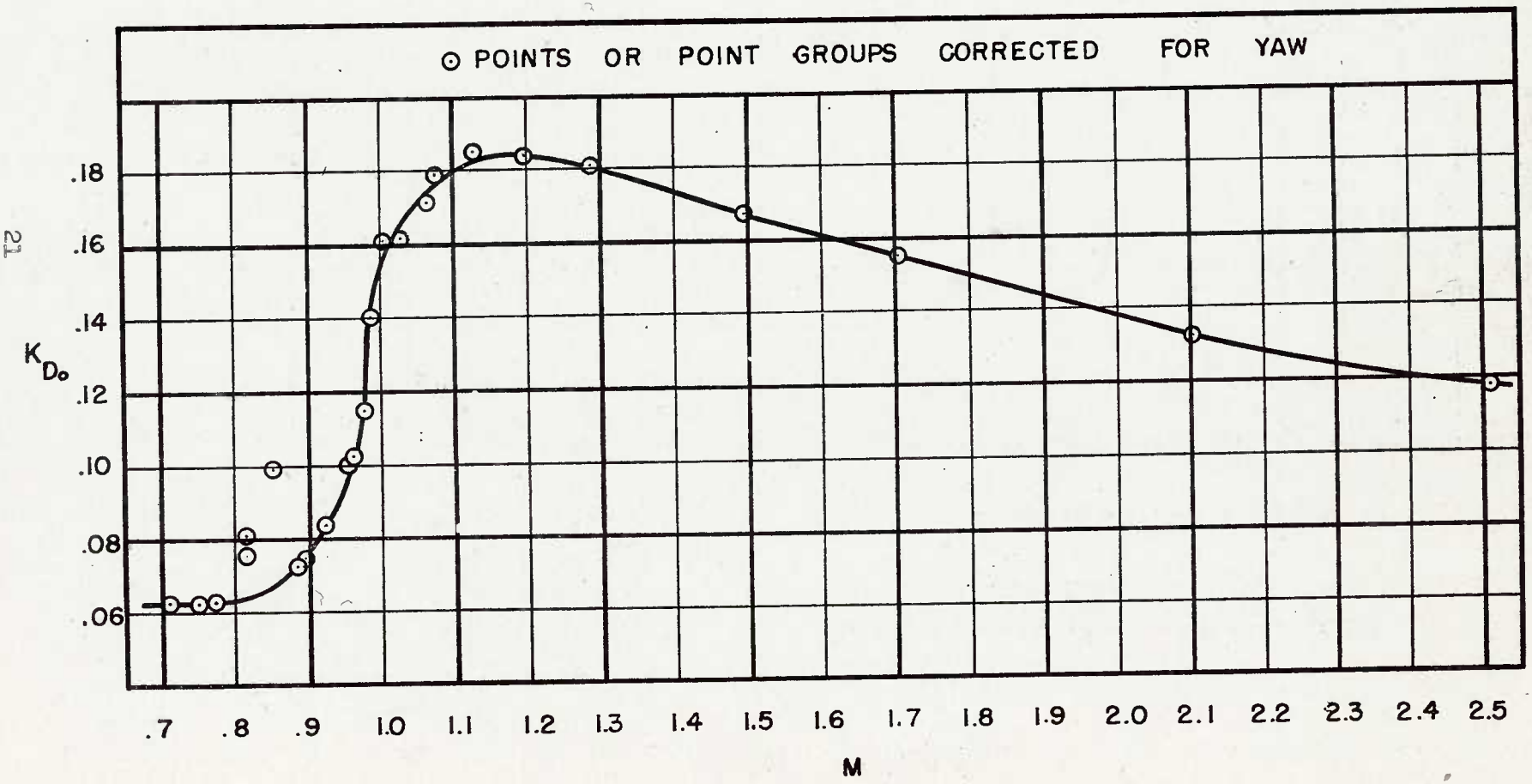

FIG 3

OVERTURNING MOMENT COEFFICIENT VS. MACH NUMBER

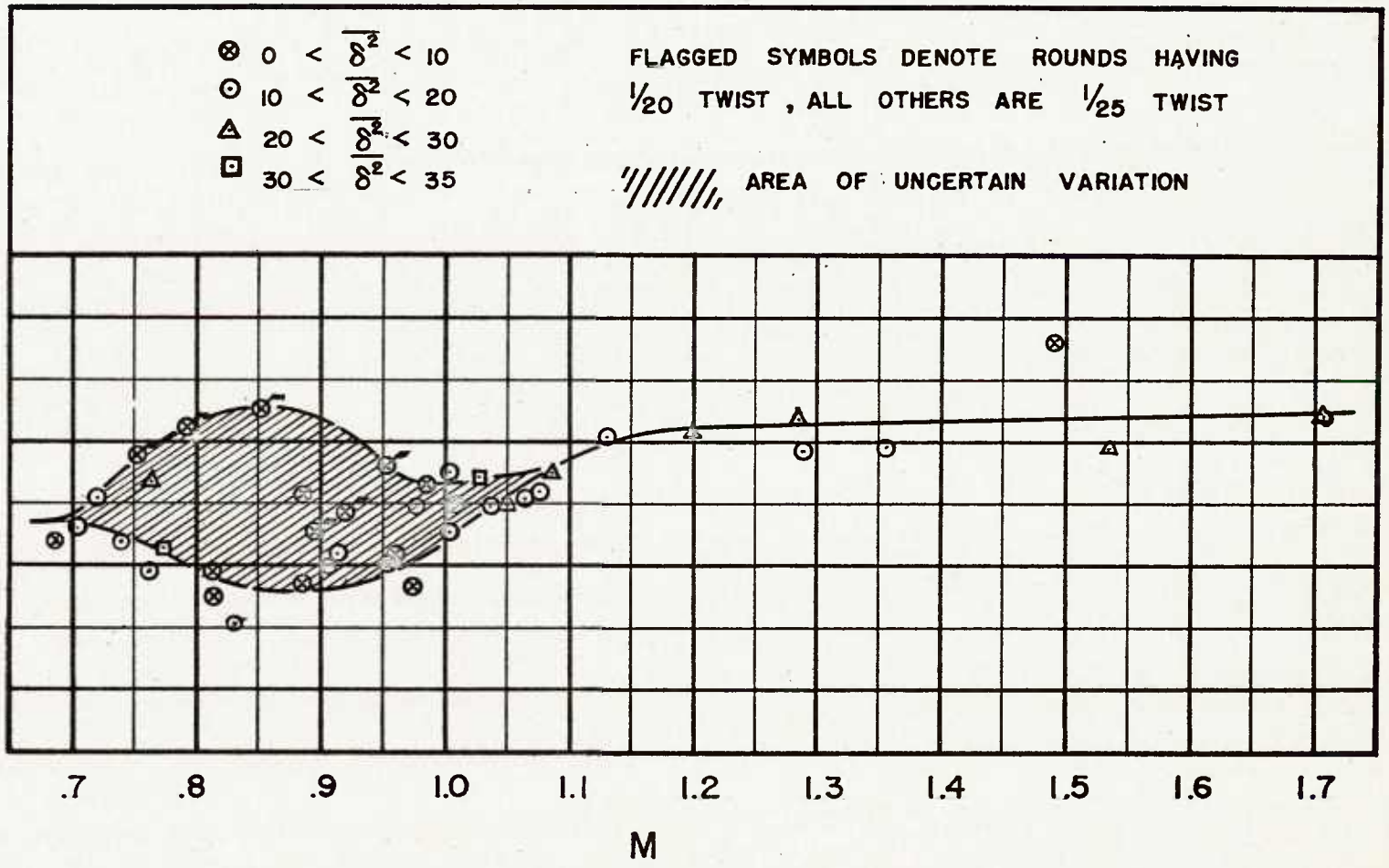

FIG. 4

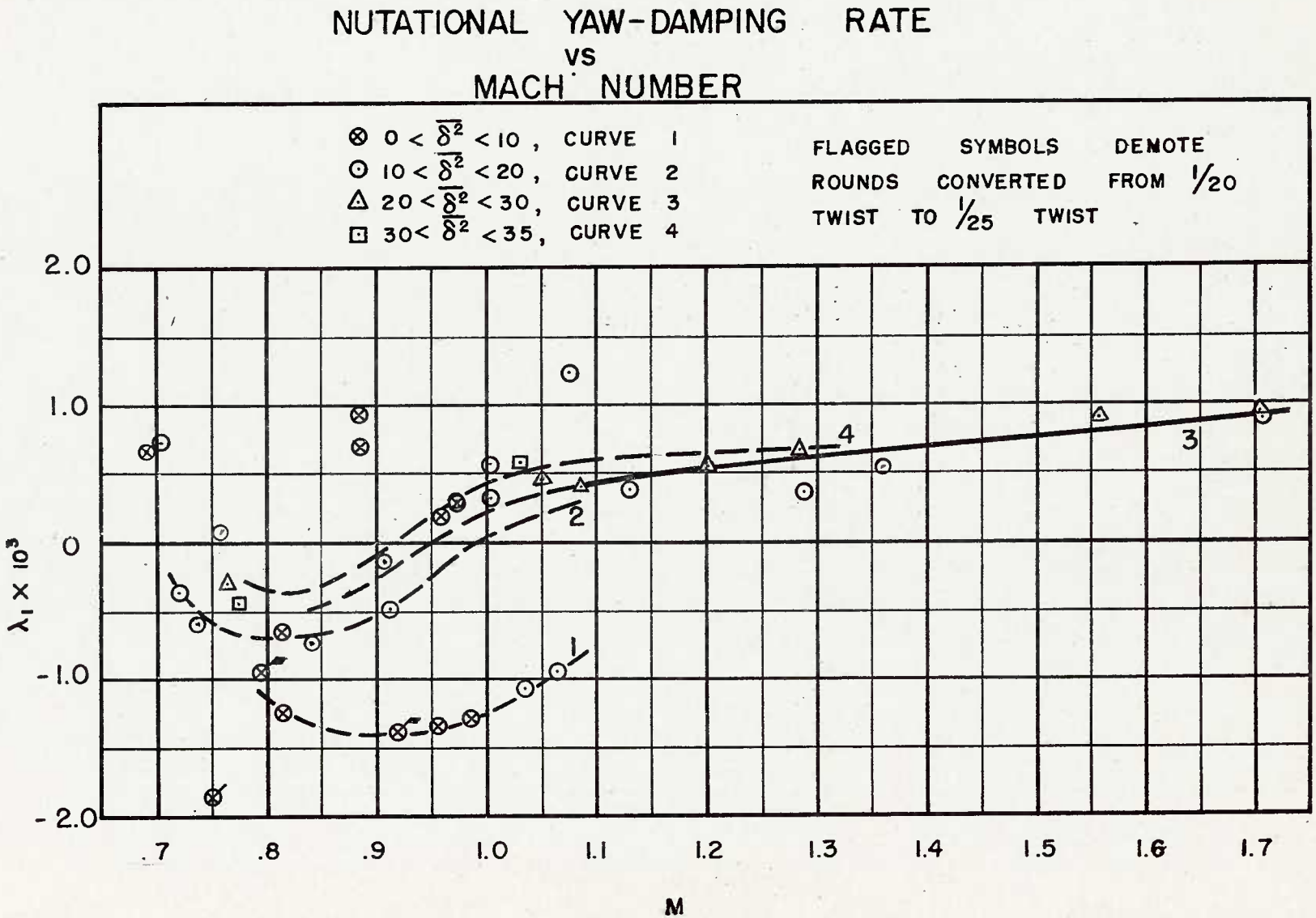
NUTATIONAL YAW-DAMPING RATE
VS
MACH NUMBER
⊗ 0 < δ̄² < 10 , CURVE 1
⊙ 10 < δ̄² < 20 , CURVE 2
△ 20 < δ̄² < 30, CURVE 3
⊡ 30< δ̄² < 35, CURVE 4
FLAGGED SYMBOLS DENOTE ROUNDS CONVERTED FROM 1/20 TWIST TO 1/25 TWIST
2.0
1.0
0
-1.0
-2.0
λ1 X 10³
.7
.8
.9
1.0
1.1
1.2
1.3
1.4
1.5
1.6
1.7
M
1
2
3
4

FIG. 5

PRECESSIONAL YAW-DAMPING RATE VS MACH NUMBER

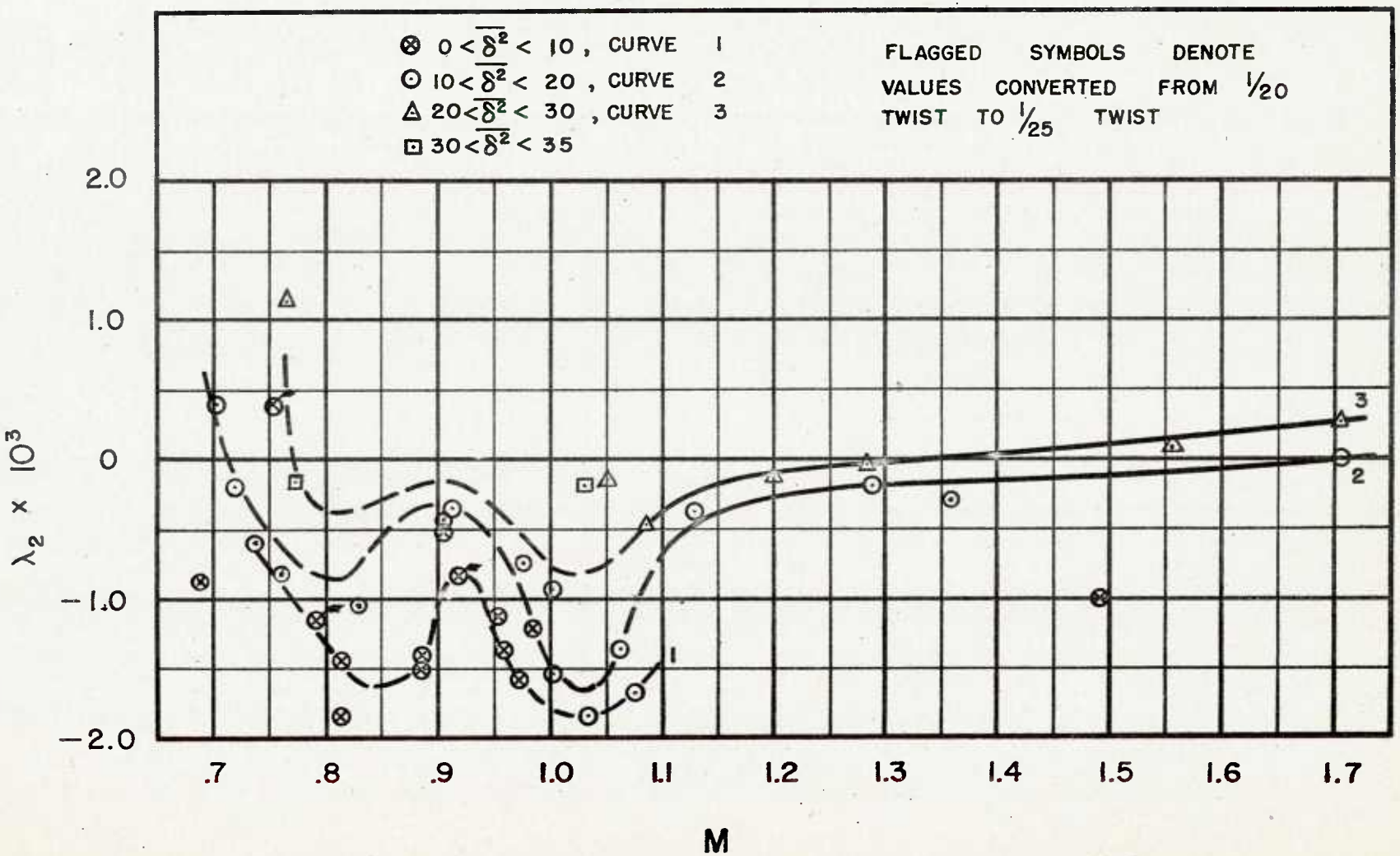

FIG. 6

POLAR YAW PLOT

ROUND 3087, M = 1.063

SPIRAL INSTABILITY

VERY SMALL NUTATIONAL ARM, GROWING PRECESSIONAL ARM

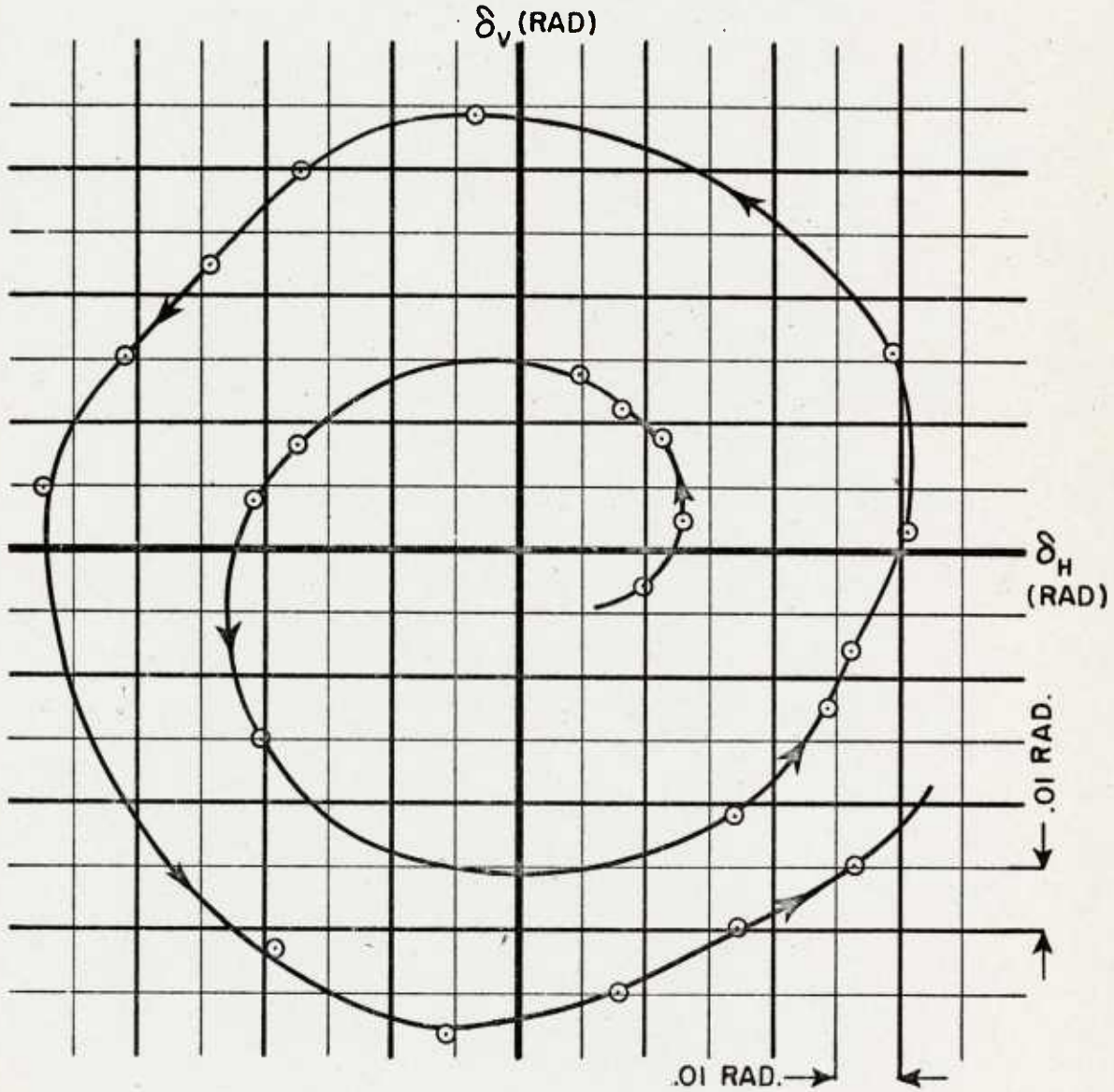

FIG. 7

AREAS OF DYNAMIC INSTABILITY

AS A FUNCTION OF MEAN SQUARED YAW AND MACH NUMBER

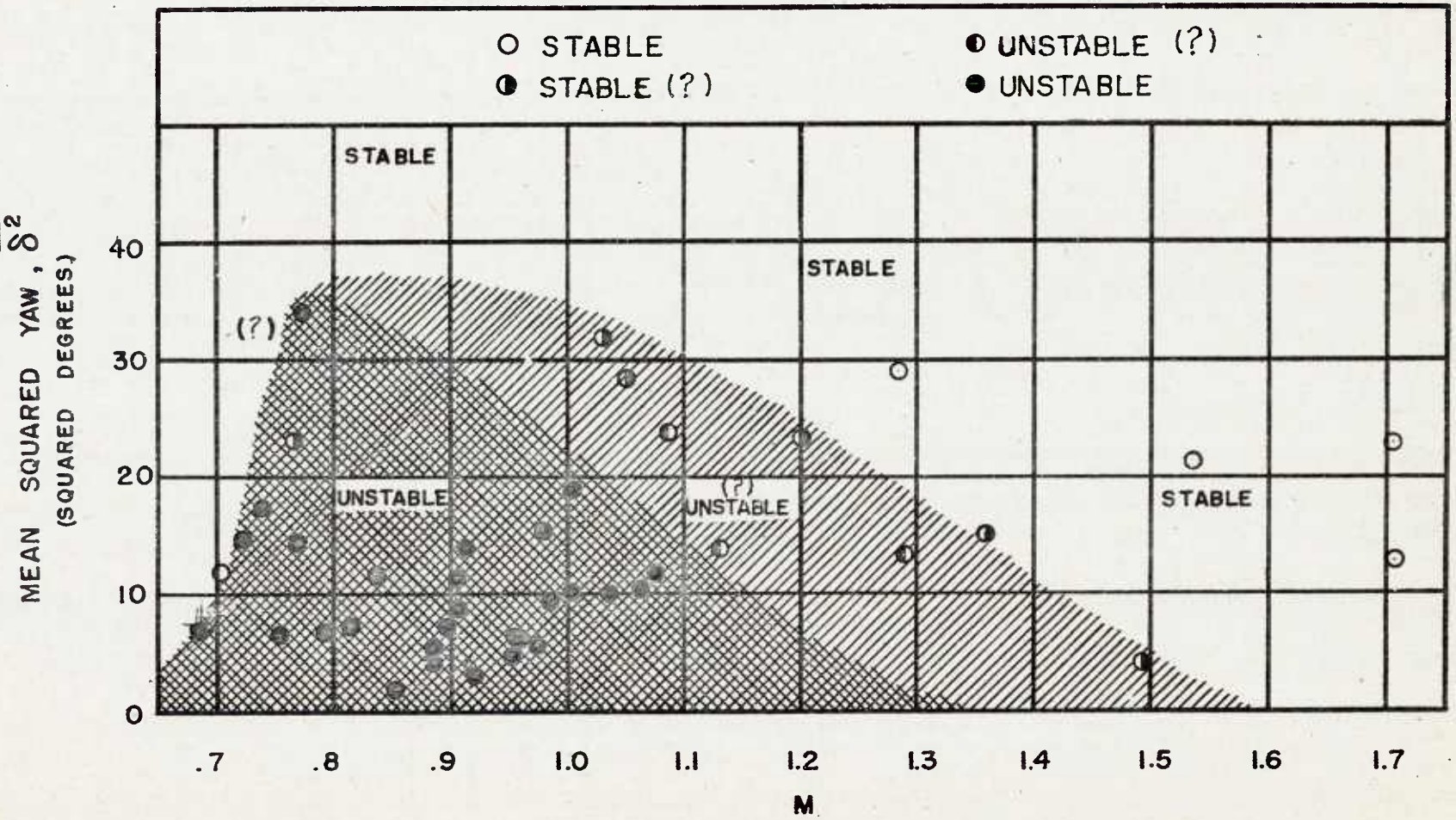

FIG 8

LIFT FORCE COEFFICIENT
VS.
MACH NUMBER

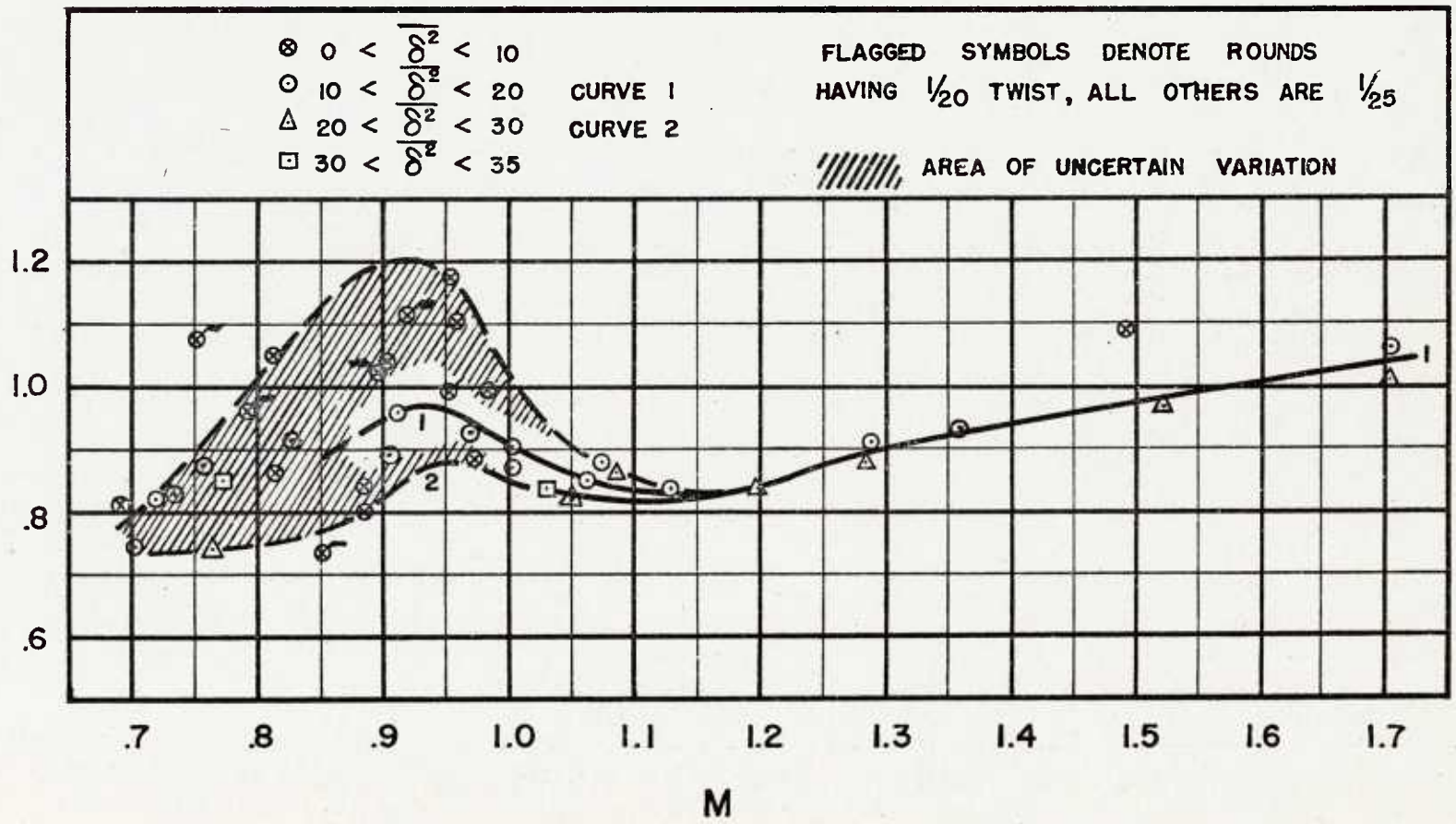

FIG. 9

YAW—DAMPING MOMENT COEFFICIENT VS. MACH NUMBER

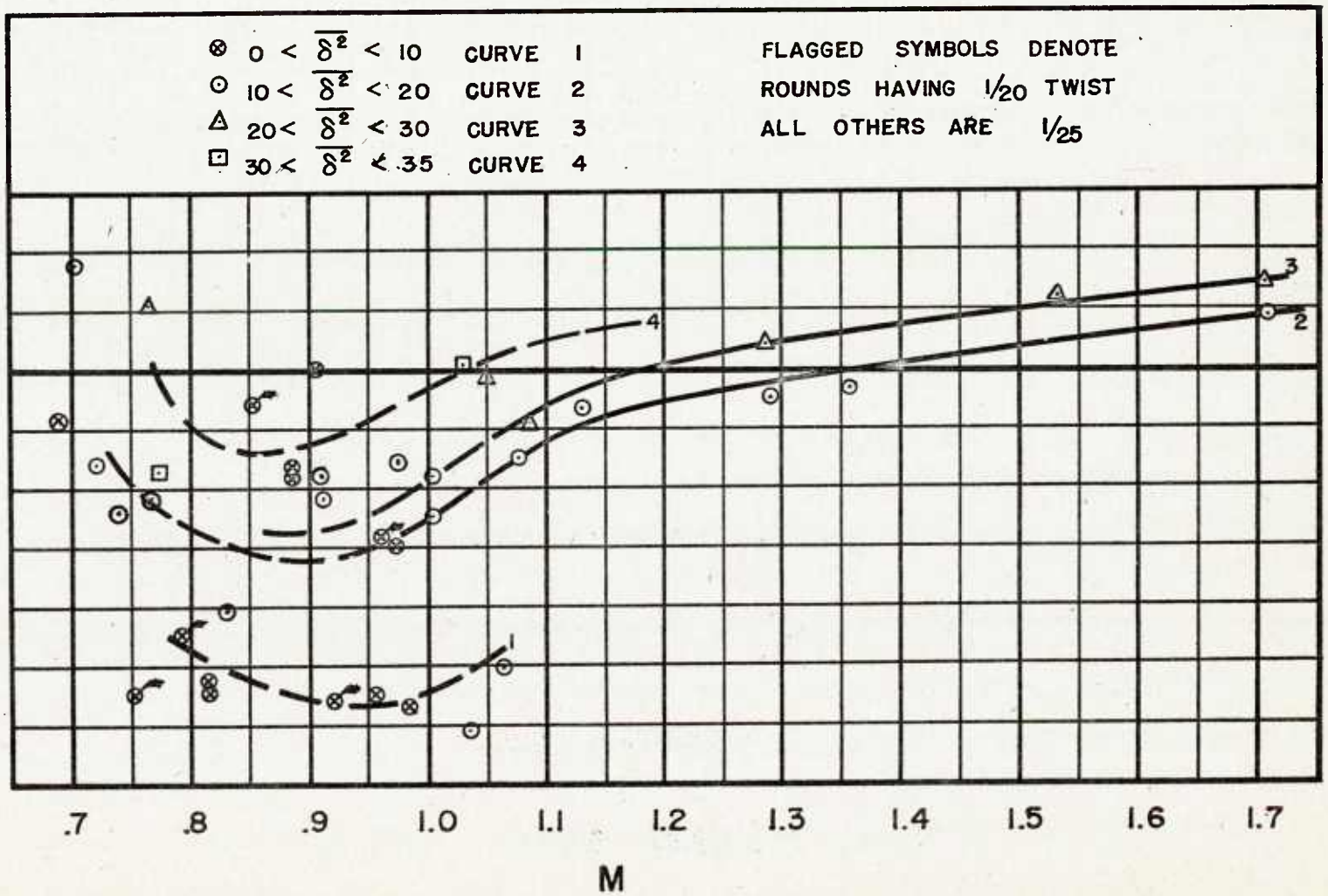

FIG. 10

MAGNUS MOMENT COEFFICIENT
VS.
MACH NUMBER

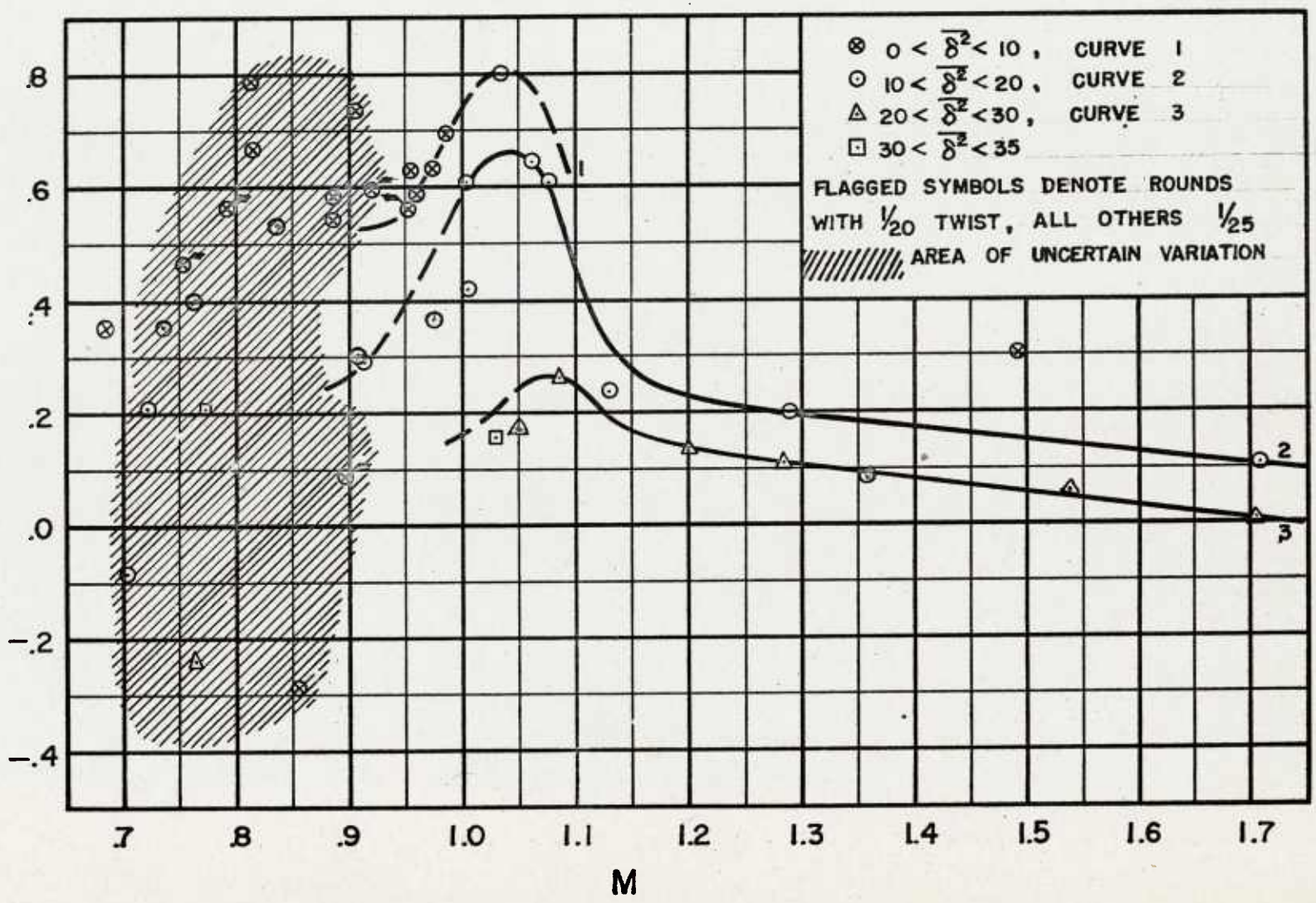

FIG. 11

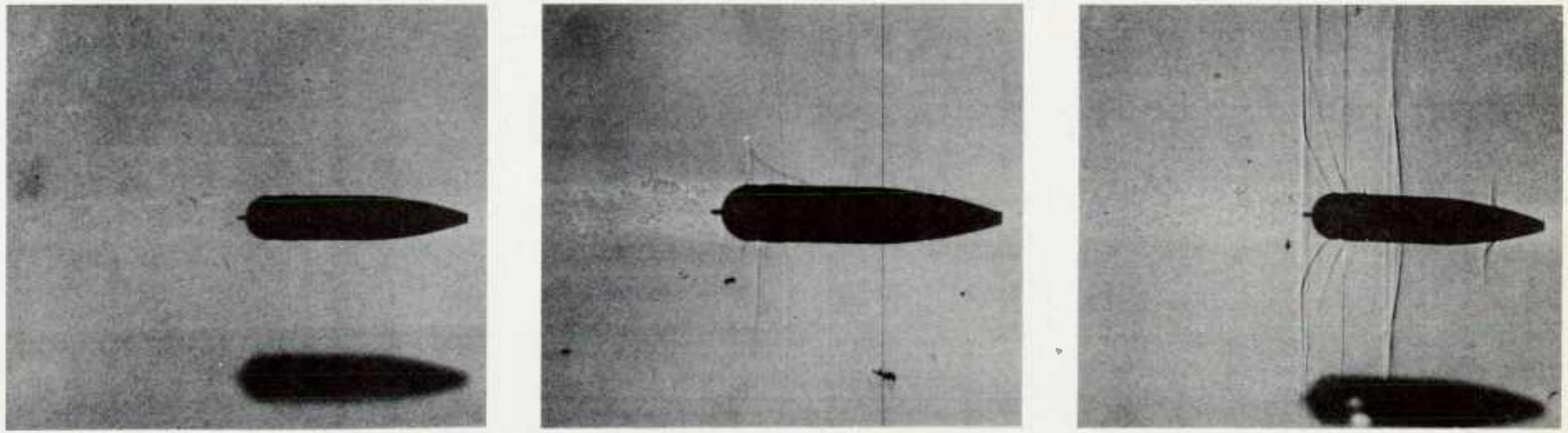

M=. 757 M=. 875 M=. 966

FIG. 12. SHADOWGRAPHS OF SHELL IN FLIGHT.

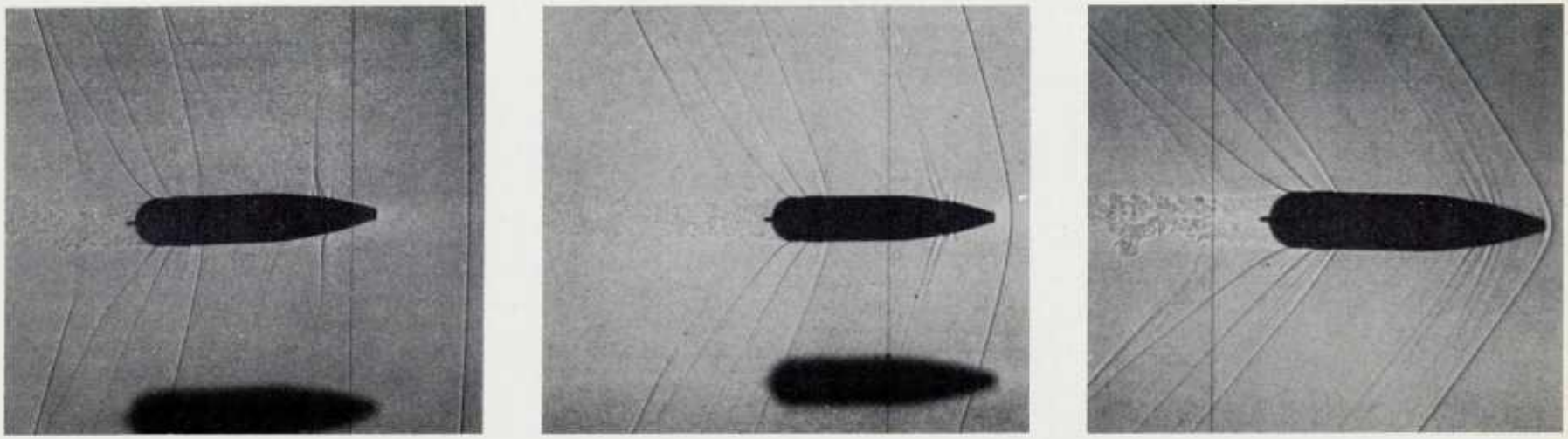

M=1.014 M=1.082 M=1.286

FIG. 13. SHADOWGRAPHS OF SHELL IN FLIGHT.

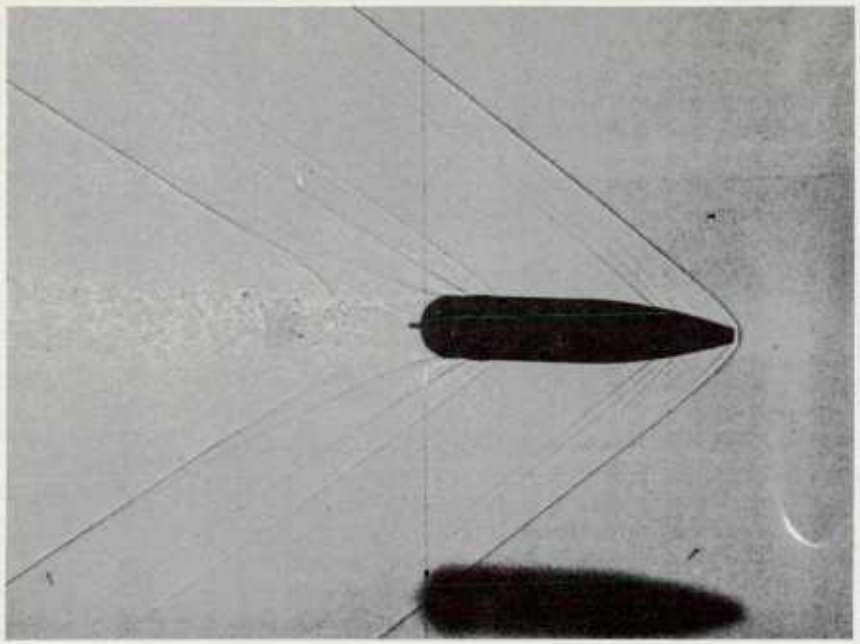

M=1. 720

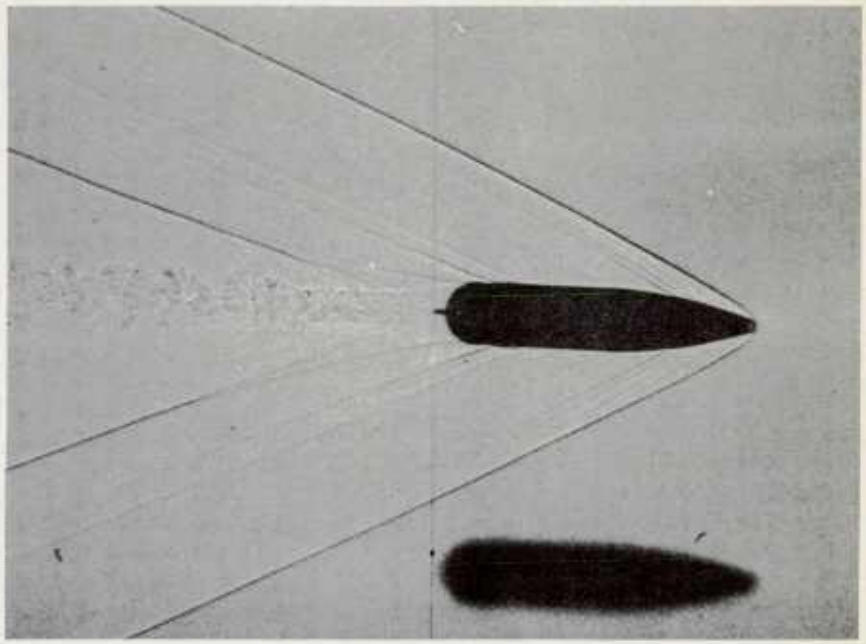

M=2. 524

FIG. 14. SHADOWGRAPHS OF SHELL IN FLIGHT.

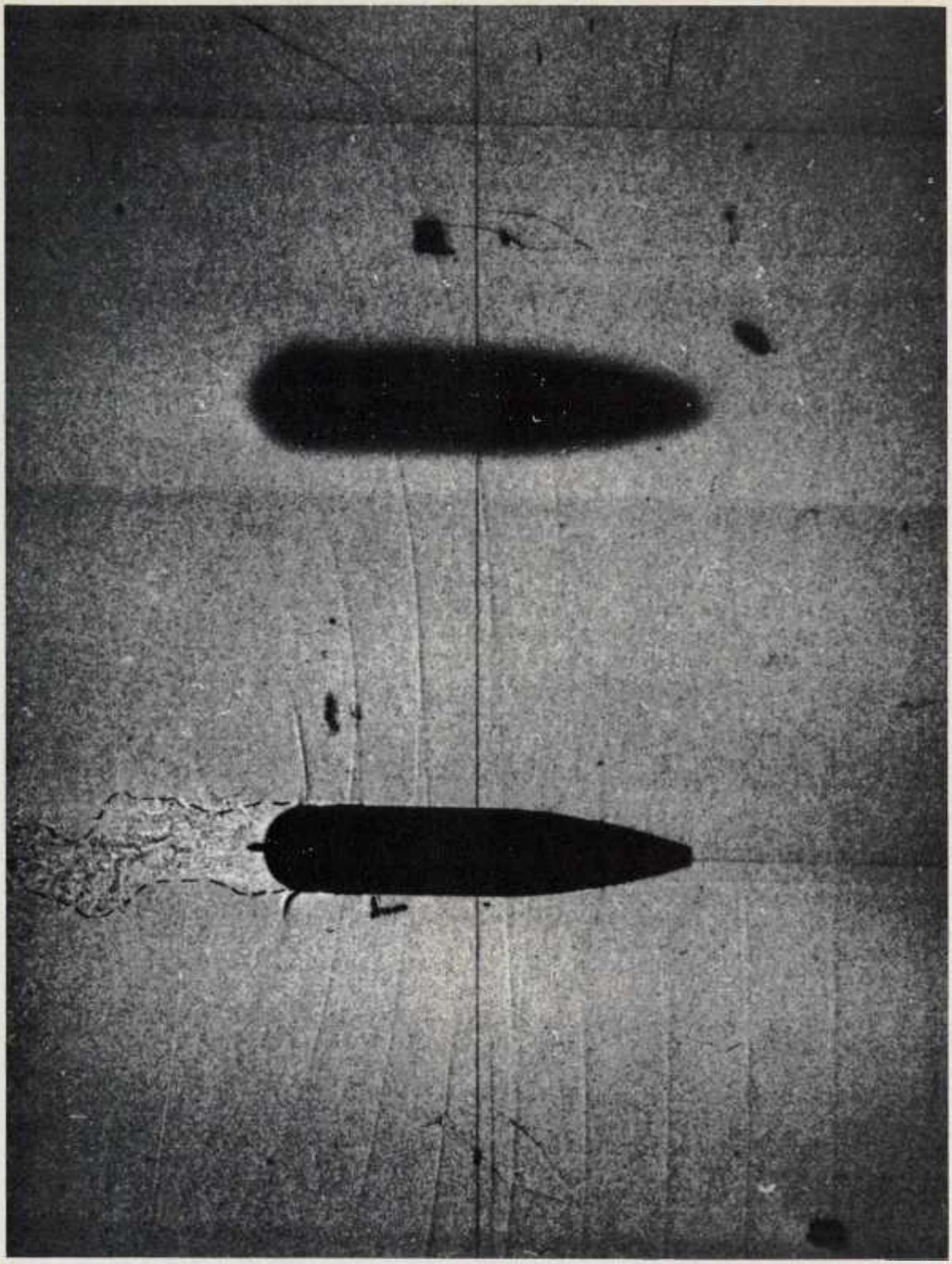

M=. 858

FIG. 15a. SHELL MOVING THROUGH SONIC FIELD GENERATED BY WAKE.

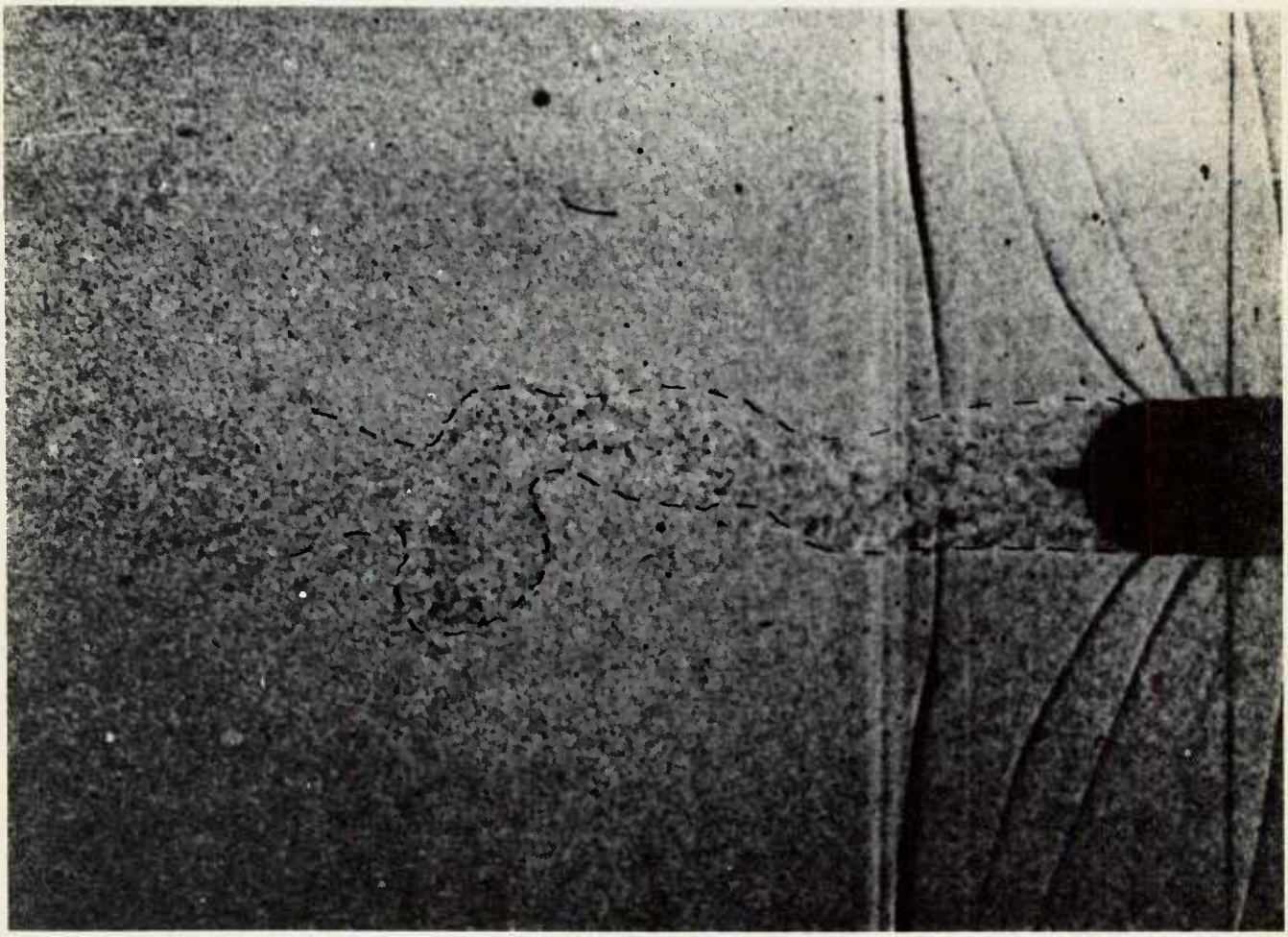

M=. 984

FIG. 15b. SHELL HAVING OSCILLATORY WAKE.

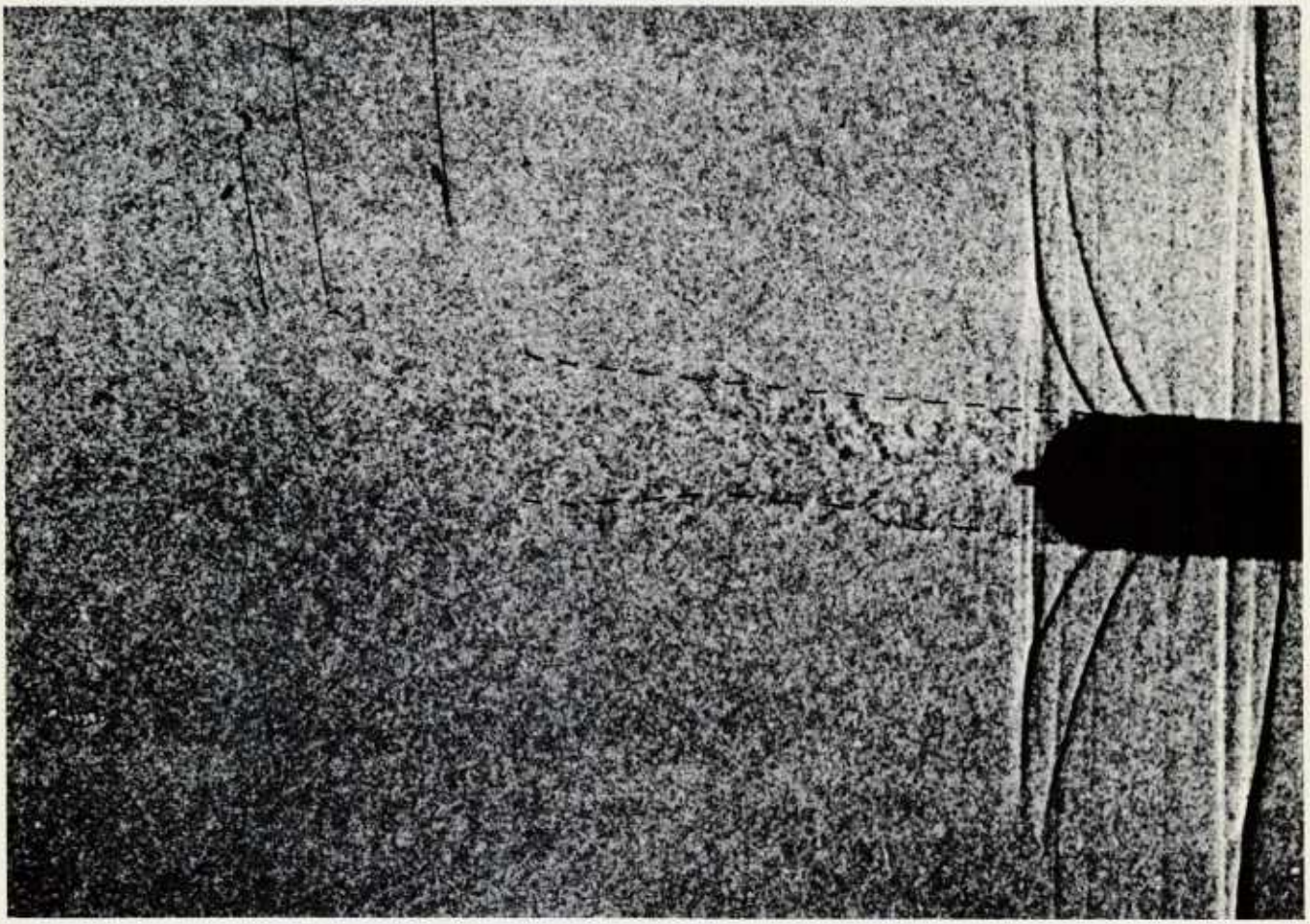

FIG. 16a. SMOOTH WAKE AT M=. 967.

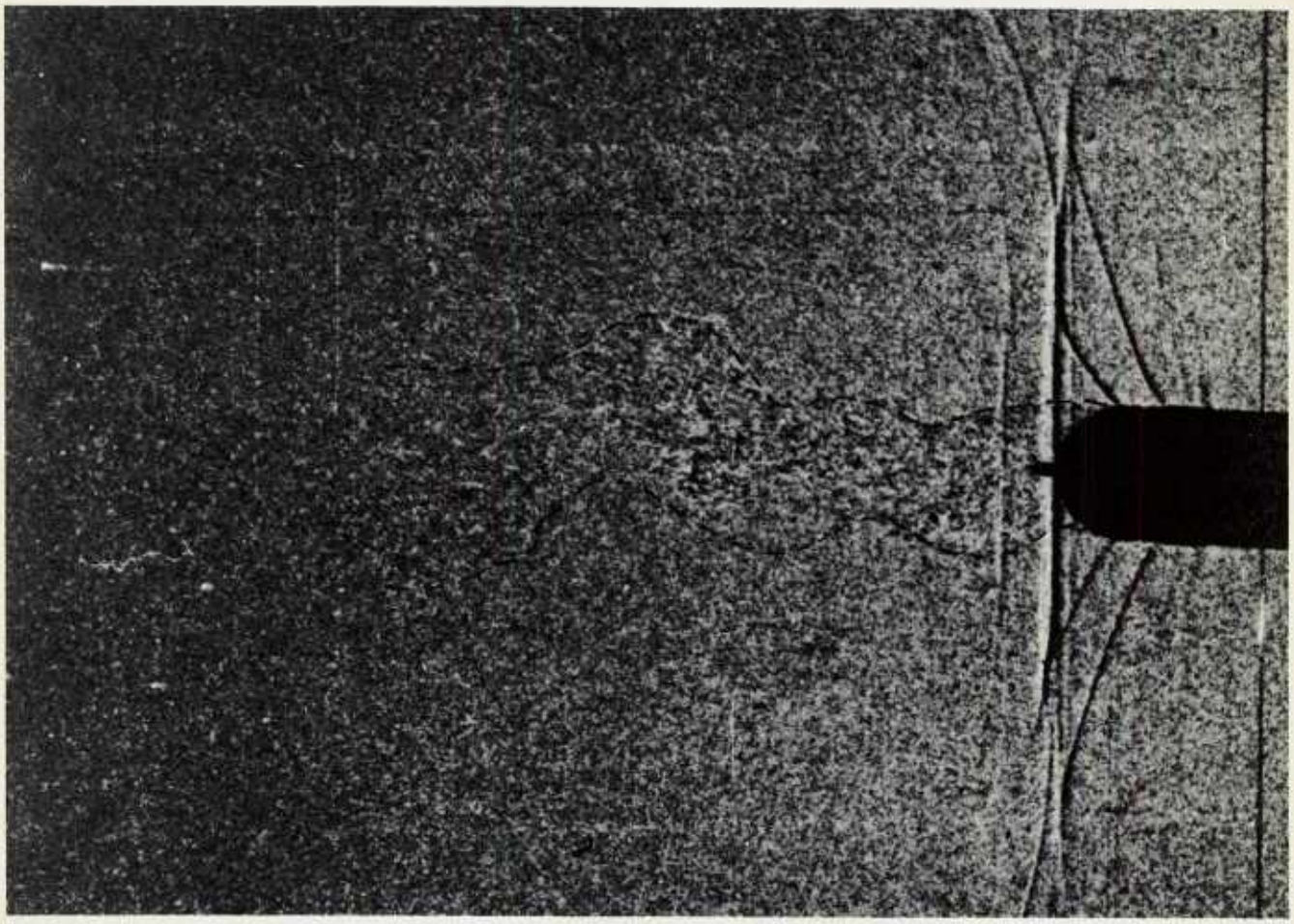

FIG. 16b. OSCILLATORY WAKE AT M=. 959.

ARMY---OS---ABERDEEN PROVING GROUND, MD.

DISTRIBUTION LIST

No. of Copies	Organization
	Chief of Ordnance Department of the Army Washington 25, D. C. Attn: ORDTB - Bal Sec
10	British Joint Services Mission 1800 K Street, N. W. Washington 6, D. C. Attn: Mr. John Izzard Reports Officer
3	Canadian Army Staff 2450 Massachusetts Avenue Washington 8, D. C.
4	Chief, Bureau of Ordnance Department of the Navy Washington 25, D. C. Attn: Re3
2	Commander Naval Proving Ground Dahlgren, Virginia
2	Commander Naval Ordnance Laboratory White Oak Silver Spring, Maryland Attn: Mr. Nestingen Dr. May
1	Superintendent Naval Postgraduate School Monterey, California
2	Commander Naval Air Missile Test Center Point Mugu, California
1	Commanding Officer U.S. Naval Air Rocket Test Station Lake Denmark, New Jersey
1	Commanding Officer and Dir. David W. Taylor Model Basin Washington 7, D. C. Attn: Aerodynamics Lab.
1	Commander Naval Air Development Ctr. Johnsville, Pennsylvania
2	Commander Naval Ordnance Test Station China Lake, California Attn: Technical Library
1	Commander Arnold Engineering Development Center Tullahoma, Tennessee Attn: Deputy Chief of Staff, R&D
4	Commander Air Research and Development Command P. O. Box 1395 Baltimore 3, Maryland Attn: Deputy for Development
5	Director Armed Services Technical Information Agency Documents Service Center Knott Building Dayton 2, Ohio Attn: DSC - SA
3	Director National Advisory Committee for Aeronautics 1512 H Street, N. W. Washington 25, D. C.
2	Director National Advisory Committee for Aeronautics Ames Laboratory Moffett Field, California Attn: Dr. A. C. Charters Mr. H. J. Allen

DISTRIBUTION LIST

No. of Copies	Organization
3	National Advisory Comm. for Aeronautics Langley Memorial Aeronautical Laboratory Langley Field, Virginia Attn: Mr. J. Bird, Mr. C. E. Brown, Dr. Adolf Busemann
1	National Advisory Comm. for Aeronautics Lewis Flight Propulsion Lab. Cleveland Airport Cleveland, Ohio Attn: F. K. Moore
2	U. S. Atomic Energy Comm. Sandia Corporation P.O. Box 5800 Albuquerque, New Mexico Attn: Mr. Wynne K. Cox
1	Commanding General Redstone Arsenal Huntsville, Alabama Attn: Technical Lib.
3	Commanding Officer Picatinny Arsenal Dover, New Jersey Attn: Samuel Feltman Ammunition Labs.
1	Commanding Officer Frankford Arsenal Philadelphia, Pennsylvania Attn: Reports Group
1	Commanding Officer Chemical Corps Chemical and Radiological Laboratory Army Chemical Center, Md.
2	Director, JPL Ord Corps Installation 4800 Oak Grove Drive Department of the Army Pasadena, California Attn: Mr. Irl E. Newlan Reports Group
6	Commanding General Ordnance Ammunition Ctr. Joliet, Illinois
1	Operations Research Office 7100 Connecticut Avenue Chevy Chase, Maryland Washington 25, D. C.
2	Applied Physics Laboratory 8621 Georgia Avenue Silver Spring, Maryland Attn: Mr. George L. Seielstad
1	Aerophysics Development Corp. P.O. Box 657, Pacific Palisades, California Attn: Dr. William Bollay
2	Armour Research Foundation Illinois Institute of Technology 35 W. 33rd Street Chicago 16, Illinois Attn: Mr. W. Casier Dr. A. Wundheiler
1	Cornell Aeronautical Lab., Inc. 4455 Genesee Street Buffalo, New York Attn: Miss Elma T. Evans Librarian
1	California Institute of Technology Guggenheim Aeronautical Lab. Pasadena, California Attn: Prof. H. W. Liepman

DISTRIBUTION LIST

No. of Copies	Organization
1	Consolidated Vultee Aircraft Corp. Ordnance Aerophysics Lab. Daingerfield, Texas Attn: Mr. J. E. Arnold
1	California Institute of Technology Norman Bridge Laboratory of Physics Pasadena, California Attn: Dr. Leverett Davis, Jr.
1	M. W. Kellogg Company Foot of Danforth Avenue Jersey City 3, New Jersey Attn: Mr. Robert A. Miller
1	University of So. California Engineering Center Los Angeles 7, California Attn: Mr. H. R. Saffell Director
1	United Aircraft Corp. Research Department East Hartford 8, Connecticut Attn: Mr. Robert C. Sale
1	University of Michigan Willow Run Research Center Willow Run Airport Ypsilanti, Michigan Attn: Mr. J. E. Corey
1	Wright Aeronautical Corp. Wood-Ridge, New Jersey Attn: Sales Dept. (Government)
1	Professor George Carrier Division of Applied Sciences Harvard University Cambridge 38, Massachusetts
1	Dr. Clark B. Millikan Guggenheim Aeronautical Lab. California Institute of Technology Pasadena, California
1	Dr. A. E. Puckett Hughes Aircraft Company Florence Avenue at Teat St. Culver City, California
1	Dr. L. H. Thomas Watson Scientific Computing Laboratory 612 West 116th Street New York 27, New York